

MicroRNA-423-5p Promotes Autophagy in Cancer Cells and Is Increased in Serum From Hepatocarcinoma Patients Treated With Sorafenib

Paola Stiuso¹, Nicoletta Potenza², Angela Lombardi¹, Ida Ferrandino³, Antonio Monaco³, Silvia Zappavigna¹, Daniela Vanacore¹, Nicola Mosca², Filomena Castiello², Stefania Porto¹, Raffaele Addeo⁴, Salvatore Del Prete⁴, Ferdinando De Vita⁵, Aniello Russo² and Michele Caraglia¹

Hepatocellular carcinoma (HCC) is the third cause of cancer-related deaths worldwide. Sorafenib is the only approved drug for patients with advanced HCC but has shown limited activity. microRNAs (miRs) have been involved in several neoplasms including HCC suggesting their use or targeting as good tools for HCC treatment. The purpose of this study was to identify novel approaches to sensitize HCC cells to sorafenib through miRs. miR-423-5p was validated as positive regulator of autophagy in HCC cell lines by transient transfection of miR and anti-miR molecules. miR-423-5p expression level was evaluated by real-time polymerase chain reaction (PCR) in sera collected from 39 HCC patients before and after treatment with sorafenib. HCC cells were cotreated with sorafenib and miR-423-5p and the effects on cell cycle, apoptosis, and autophagy were evaluated. Secretory miR-423-5p was upregulated both *in vitro* and *in vivo* by sorafenib treatment and its increase was correlated with response to therapy since 75% of patients in which an increase of secretory miR423-5p was found were in partial remission or stable disease after 6 months from the beginning of therapy. HCC cells transfected with miR-423-5p showed an increase of cell percentage in S-phase of cell cycle paralleled by a similar increase of autophagic cells evaluated at both fluorescence activated cell sorter (FACS) and transmission electron microscopy. Our results suggest the miR423-5p can be used as a useful tool to predict response to sorafenib in HCC patients and is involved in autophagy regulation in HCC cells.

Molecular Therapy—Nucleic Acids (2015) 4, e233; doi:10.1038/mtna.2015.8; published online 17 March 2015

Subject Category: siRNAs, shRNAs, and miRNAs Therapeutic proof-of-concept

Introduction

Hepatocellular carcinoma (HCC) is among the most common malignancies worldwide, with approximately more than 500,000 new patients diagnosed each year; however, significant regional differences in the incidence of HCC are observed because of the frequency of the different etiological factors involved in HCC development.¹ Despite major efforts to improve diagnosis and treatment of HCC, therapeutic options remain limited; treatment options depend on the stage of the disease and the extent of liver dysfunction and cirrhosis.² Therefore, targeting the key-role genes and pathways has increasingly gained attention. Presently, molecular mechanisms leading to malignant transformation of hepatocytes as well as development and progression of HCC still remain largely unclear. The mitogen-activated protein kinase (MAPK) pathway (including RAS, BRAF, MEK1/2, and extracellular-signal-regulated kinase (ERK 1/2 proteins cascades) has emerged as a major signaling pathway, involved in the control of cell growth, apoptosis, proliferation, and migration in most cancers. It has also established that alternative mechanisms of regulation of cell death exist and one of these is autophagy occurrence that has been also recently correlated to the activity of anticancer agents.^{3,4} Recently, sorafenib, an oral multikinase inhibitor targeting RAF

kinases among other cellular kinases, has been demonstrated to be effective in HCC.⁵ Ablative therapy, surgical resection, or liver transplantation are the first-line treatments for patients affected by HCC.⁶ Nonetheless, both advanced tumor stage and poor liver function preclude the majority of patients from these surgical interventions. In addition to this obstacle, transplantation is indicated only for early small HCC, and its application is limited by the availability of liver grafts.⁷ Therefore, there is an urgent need to develop an effective systemic therapy for patients with advanced HCC.⁸ In the last years, many advances in the knowledge of the molecular mechanisms that govern tumor development and progression have been made.⁹ More recently, single agent sorafenib has shown to prolong the overall survival (OS) of patients with advanced HCC in the pivotal phase 3 Sorafenib HCC Assessment Randomized Protocol and Oriental study.⁷ Currently, sorafenib is the only approved targeted therapy for patients with advanced HCC.

MicroRNA (miRNA) is a class of single-stranded, 19–25 nucleotides in length, noncoding RNA molecules in eukaryotes. Binding to the 3'-untranslated region (3'-UTR) of target mRNAs, miRNAs regulate the translation and degradation of its target mRNAs and thus influence gene expression.^{10,11} More and more evidence has shown that miRNAs are strongly related to oncogenesis.^{12,13} It has been shown that miRNAs play critical

The first two authors contributed equally to this work.

¹Department of Biochemistry, Biophysics and General Pathology, Second University of Naples, Naples, Italy; ²Department of Environmental, Biological and Pharmaceutical Sciences and Technologies, Second University of Naples, Naples, Italy; ³Department of Biology, University "Federico II" of Naples, Naples, Italy; ⁴Medical Oncology Day Hospital Unit, San Giovanni di Dio Hospital, Naples, Italy; ⁵Department of Clinical and Experimental Medicine and Surgery, Second University of Naples, Naples, Italy Correspondence: Michele Caraglia, Department of Biochemistry, Biophysics and General Pathology, Second University of Naples, Naples, Italy. E-mail: michele.caraglia@unina2.it

Keywords: Autophagy; hepatocellular carcinoma; miRNA; prognosis; treatment

Received 18 December 2014; accepted 11 February 2015; published online 17 March 2015. doi:10.1038/mtna.2015.8

roles in tumor suppression or carcinogenesis by regulating gene expression at post-transcriptional levels.¹⁴ On this light, miRNAs and their inhibitors are emerging as useful tool in order to control neoplastic diseases.¹⁵ Moreover, a large number of tumor-derived microRNAs exist in human serum/plasma in a stable, reproducible, and consistent form, which thus can serve as potential biomarkers for blood-based detection of human cancers diagnosis and/or prognosis.^{13,14,16} Indeed, a recent study screened a plasma microRNA panel and identified several miRNAs that showed high effectiveness and accuracy in HCC diagnosis.¹⁷ Such inspiring results pushed forward the development of the early detection of HCC based on miRNAs.

The differential expression of miRNAs in HCC cells compared with their expression in normal hepatocytes indicates potential values of miRNA detection in HCC diagnosis and prognosis prediction. For example, HCCs can be divided into three main clusters based on miRNA profiling each of one with different clinical outcome.¹⁸ Deregulation of miRNAs significantly contributes to the development of HCC. miRNAs mainly function to downregulate the expression of targeted genes. However, they may have other yet unknown functions including the activation of gene transcription. The discovery of new types or novel functions of miRNAs provides us with more and deeper insights into the molecular mechanism underlying the pathogenesis of HCC.¹⁹ On the other hand, miRNA expression profiles altered in HCC paves the way to early detection and treatment of HCC. With the advantage of target multiple genes simultaneously, miRNAs as therapeutic targeting would be more efficient than other single-gene targeted therapeutics such as RNAi-based therapy, thus representing a new avenue for the development of anti-HCC treatments. Based on this evidence, we have evaluated in HCC cells and in a series of HCC patients the effects of sorafenib on secreted miRNAs paying attention to miR-423-5p. Thereafter, we have studied the biological activity of this miRNA in HCC cells disclosing its role in the regulation of cell cycle and autophagy occurrence.

Results

Secretory miR-423-5p is upregulated *in vitro* in response to sorafenib treatment

Recent studies demonstrated that miRNAs are secreted after they are contained in RNase-resistant lipid vesicles, such as exosomes and apoptotic bodies via an exosome-dependent pathway. On this light, a screening of secretory miRNAs was performed on cell culture medium after sorafenib treatment.^{20,21} We have firstly evaluated the antiproliferative effects of Sorafenib on two different HCC cell lines (HepG2 and HuH-7) using concentrations of sorafenib, ranging from 0.1 to 50 $\mu\text{mol/l}$. Cell viability was evaluated with MTT assay as explained in “Materials and Methods” section. Sorafenib induced 50% of growth inhibition at 72 hours (IC₅₀) at the concentration of 5 and 6 $\mu\text{mol/l}$ in HepG2 and HuH-7, respectively. (Figure 1) Subsequently, HepG2 cell culture supernatants were collected 72 hours after growth in standard conditions or in the presence of 5 $\mu\text{mol/l}$ sorafenib and the expression of 84 miRNAs, generally detectable in serum, plasma, and other body fluids, was profiled by RT-qPCR arrays. Most of analyzed miRNAs were found decreased in the medium of cells after sorafenib

treatment (61 miRNAs out of 84) (Figure 2). Among extracellular miRNAs found increased in response to sorafenib treatment, miR-423-5p was at the top; so, we decided to focus our attention on this miRNA. A time course analysis was performed and revealed that an increased level (ranging from 1.4- to 1.8-fold change) of extracellular miR-423 was detectable also 24 and 48 hours after sorafenib treatment (Figure 3a). The effect of sorafenib treatment on the level of secretory miR-423 was also investigated for HuH-7. In this case, the increase of miR-423 was higher than that one observed for HepG2 cells, ranging from 4- to 30.8-fold change (Figure 3b) and highlighting a kinetic of miR-423 upregulation. Taken together, these data clearly showed a correlation between sorafenib treatment and the accumulation of extracellular miR-423.

Increased miR-423-5p secretion was correlated to increased intracellular ceramide production

The secretion of miRNAs is triggered by the increase of cellular amount of ceramide, a bioactive sphingolipid, whose synthesis is tightly regulated by neutral sphingomyelinase 2 (nSMase2).²² On the basis of these findings, we have evaluated the effect of sorafenib addition to HCC cells on the intracellular levels of ceramides. We have found that 72-hour 5 $\mu\text{mol/l}$ sorafenib treatment of HCC HepG2 cells increased the production of secondary ceramides metabolites in cell medium by using MALDI-TOF spectroscopic techniques (Figure 4). A series of sphingolipid components in the mass range 600–750 Da were observed in the cells treated with sorafenib. In details, an increase of the following long chain ceramides was recorded: (i) Cer(d14:1(4E)/26:0(2OH)) (637.92 C₄₀H₇₉NO₄); (ii) PE-Cer(d14:1(4E)/20:1(11Z)) (659 C₃₆H₇₁N₂O₆P); (iii) PE-Cer(d16:1(4E)/24:0(2OH)) (760 C₄₂H₈₅N₂O₇P). Moreover, a significant increase of diacylglycerophosphoserine (703 C₃₆H₆₆NO₁₀P) was also recorded. Based on these findings, it can be hypothesized that a change in ceramide biosynthesis pathway was elicited by sorafenib and this can be associated to an increased secretion of miRNAs in exosomes.

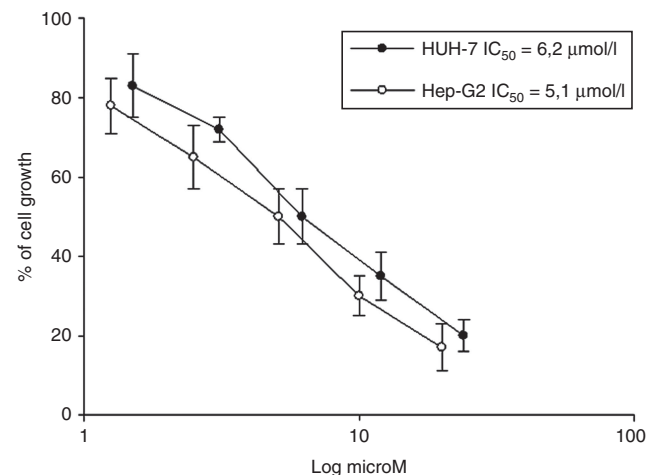


Figure 1 Dose–response effects of sorafenib on different cell lines. HepG2 and HuH7 cells were seeded and treated with different concentrations of sorafenib for 72 hours and thereafter cell viability was assessed as described in “Materials and Methods”. The experiment was repeated three times and the results are the mean of the different data. Bars represent standard deviations.

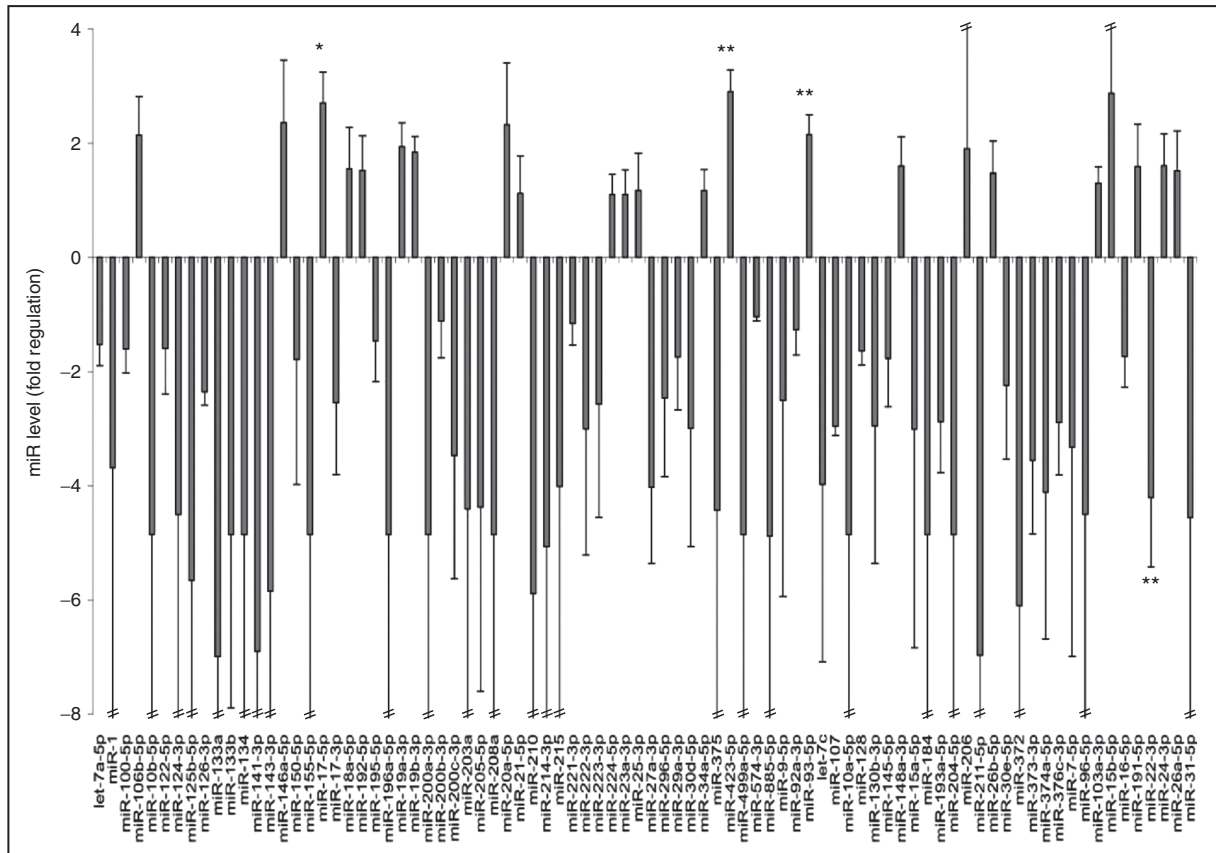


Figure 2 miRNA profiling. Fold regulation of miRNA levels detectable in the medium of sorafenib-treated cells versus nontreated cells. *P* values at Student's *t*-test were **P* < 0.05, ***P* < 0.01, or ****P* < 0.001.

miR-423-5p serum levels were upregulated by sorafenib treatment in HCC patients

Recently, plasma levels of miRNAs have emerged as potential biomarkers for various pathological conditions such as cancers.^{13,23} Based upon our *in vitro* results on both medium miRNA levels and ceramide biosynthesis, we have hypothesized that also in HCC patients serum miR-423 levels could be modulated by sorafenib treatment. Thirty-nine patients were enrolled and treated with sorafenib for advanced HCC. Serum was collected before the beginning of the treatment and 10 days from therapy start as described in “Materials and Methods”. miR-423 was quantified in serum samples with RT-qPCR technique. MiR-423-5p was detectable in all samples and its mean value was found 2.1-fold higher after sorafenib therapy (Figure 5). Overall, the results from *in vitro* modulation of miR-423 levels in HCC cell lines correlated with the clinical observations on an increase of miR-423 serum levels after sorafenib therapy in HCC patients and spread light on the potential use of miRNA 423-5p as a predictive marker of response to sorafenib in HCC patients.

Effects of miR-423-5p on cell proliferation and distribution in cell cycle

To evaluate the role played by miRNA 423-5p on the regulation of HCC cell proliferation, we have performed a transient transfection of HuH-7 cells with either miR 423-5p or anti-miR 423-5p and the effects on miRNA levels were assessed

with RT-qPCR. The overexpression of miR-423 was higher after 72 hours from the transfection with mimic while inhibitor significantly decreased miRNA 423-5p levels. In order to evaluate the effects of miR 423-5p on the distribution of HCC cells in cell cycle, we performed a FACS analysis after propidium iodide labeling, as described in “Materials and Methods”, on HuH-7 transfected with either miR 423-5p mimic or inhibitor after 72 hours from the transfection. miR 423-5p mimic induced a significant increase of S phase about 2.7-fold if compared to the cells transfected with an unrelated sequence (Ctrl-miRNA) and an about 3.6-fold decrease of cells in G₂/M phase. Sorafenib treatment of HuH7 cells transfected with mimic miR 423-5p induced an additional increase of cells in G_{0/1} phase (Figure 6a). These data suggested that HuH7 cells failed to efficiently transit from S to G₂/M phase after 72 hours from the transfection with miR 423-5p mimic. On the other hand, transfection with inhibitor did not induce significant effects on HCC distribution in the different phases of cell cycle.

On the bases of these results, we studied the effects of miR 423-5p on two cyclin-dependent kinase inhibitors p21 and p27, negative check-point regulators of the cell cycle, involved in the transition from G₀/G₁ to S phase. After 72 hours from the transfection, miR 423-5p mimic induced a significant increase in p27 expression (about sixfold, *P* < 0.001 versus control), and a slight increase of p21 expression as evaluated by western blotting assay. (Figure 6b)

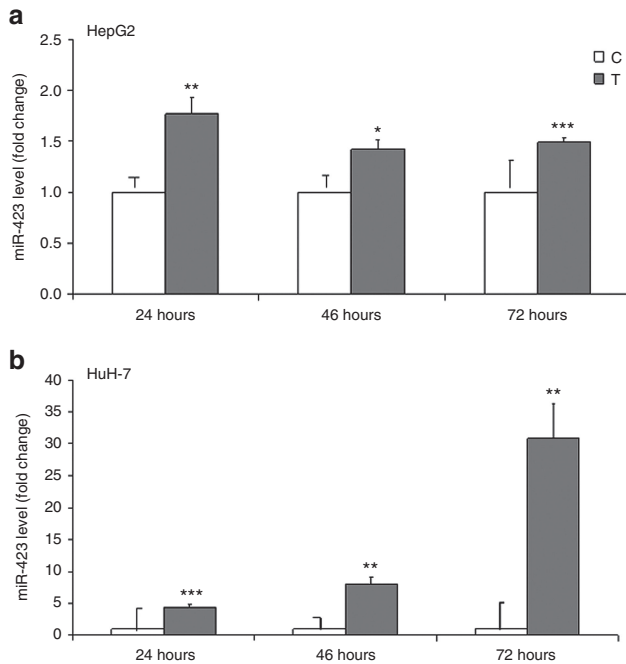


Figure 3 Secretory miR-423. Medium conditioned by HepG2 (a) and HuH-7 (b) cells were collected at the indicated time after culturing them in standard condition (C, control) or with 5 $\mu\text{mol/l}$ sorafenib (T, treatment). Relative miR-423 level was determined by quantitative real-time polymerase chain reaction as described. *P* values at Student's *t*-test were **P* < 0.05, ***P* < 0.01, or ****P* < 0.001.

Therefore, the delay in G_0/G_1 -S phase progression occurred together with an increase in p27 and, at a lesser extent, in p21 protein expression.

In **Figure 6**, we reported the effects of the overexpression of miR 423-5p on two key molecules involved in the regulation of both cell proliferation and survival, MAPK (Erk-1 and Erk-2) and AKT. After 72 hours, miR 423-5p mimic decreased both pErk-1/2 and AKT expression as compared to both control and unrelated sequence mimic (**Figure 6b**). On the basis of above results, we have studied apoptosis occurrence in transfected cells using FACS analysis after double labeling with propidium iodide (PI) and annexin V fluorescein isothiocyanate and we have found no evidence of apoptosis (data not shown). Therefore, we used miRanda and TargetScan to identify target genes of miR 423-5p and identified potential candidate targets related to cell death. The analysis revealed that ATG7 (an autophagy vacuole formation protein) is a putative gene target of miR 423-5p. On this light, we have evaluated the expression of ATG7 and we have found that the expression of ATG7 was about onefold increased in HuH-7 cells transfected with miR 423-5p mimic; on the other hand, HuH-7 transfected with miR-423-5p inhibitor showed a significant decrease of ATG7 suggesting that the latter is an indirect target of miR 423-5p (**Figure 7a**). Moreover, LC3-II protein, the phospho-ethanolaminated and truncated form of the autophagosome protein LC3-I, was increased by cell transfection with miR423-5p mimic if compared to the control (HuH7 transfected with Ctrl- miRNA) (1.5-fold, *P* < 0.001), (**Figure 7a**).

miRNA 423-5p induces autophagy in HCC cells

On the basis of the above reported results, we have studied the alternative autophagy cell death mechanism. The autofluorescent probe monodansylcadaverine (MDC) is a selective marker of autophagic vacuoles and especially of autolysosomes. On this light, we have evaluated MDC uptake in cells transfected or not with miR 423-5p mimic. **Figure 7b** shows the quantitative evaluation of MDC staining performed by FACS and expressed as % mean fluorescence intensity (MFI) of control (**Figure 7b**). We have found that miR 423-5p mimic induced a significant increase in autophagic vacuoles formation in HuH-7 (about 60 % of both parental and scramble transfected cells) while the transfection of the inhibitor did not induce any change in autophagic vacuoles formation in HuH-7 cells (**Figure 7b**). Interestingly, the transfection of HuH-7 cells with either mimic or inhibitor did not substantially change the effect induced by treatment of HCC cells with sorafenib as MFI was increased of about 25–30% in all the experimental conditions (**Figure 7b**).

On the basis of these results, we have evaluated the autophagy occurrence at transmission electron microscopy (TEM). Not transfected HuH-7 cells exhibited the ultrastructural morphology of cytoplasm, organelles, and nuclei similar to that one of normal hepatocytes (**Figure 8a,b**). The most prominent morphological changes in cells transfected with miR 423-5p were formation of abundant autophagic vacuoles sequestering cytoplasm and organelles, such as mitochondria and endoplasmic reticulum. Double-membranes, giant autophagosomes, filled with degraded organelles and autolysosomes were frequently observed. Autophagosomes are derived from isolated membranes that, possibly, originated from ribosome-free endoplasmic reticulum. These isolated membranes elongate and curve at both ends to form C-shaped structures and double-membrane vacuoles.⁴ In **Figure 8c,d**, the images showed typical C-shaped double-membrane structures, double-membrane autophagosomes, and lysosomes fusing with autophagosomes. TEM, the standard method to detect autophagy, was performed to detect the formation of autophagosomes, demonstrating that miR 423-5p induced autophagy in HuH-7 cells.

Discussion

The analysis of circulating miRNAs has showed that they can have a biological role and can be used as diagnostic, prognostic, and predictive biomarkers and also studied as therapeutic targets.¹⁶ In fact, several serum miRNAs were significantly overexpressed in patients if compared to healthy subjects in a study in ovarian cancer.²³ Recently, it was demonstrated that serum miRNA can be useful for the diagnosis of HCC. Tan *et al.*²⁵ identified eight miRNAs (hsa-miR-206, hsa-miR-141-3p, hsa-miR-433-3p, hsa-miR-1228-5p, hsa-miR-199a-5p, hsa-miR-122-5p, hsa-miR-192-5p, and hsa-miR-26a-5p) and constructed a miRNA set that provides high diagnostic accuracy for HCC that can be used to differentiate HCC patients from healthy and cirrhosis patients. Several findings exist about the correlation of different serum miRNA and the diagnosis of HCC differentiating the latter with nontumoral disease of the liver such as cirrhosis and

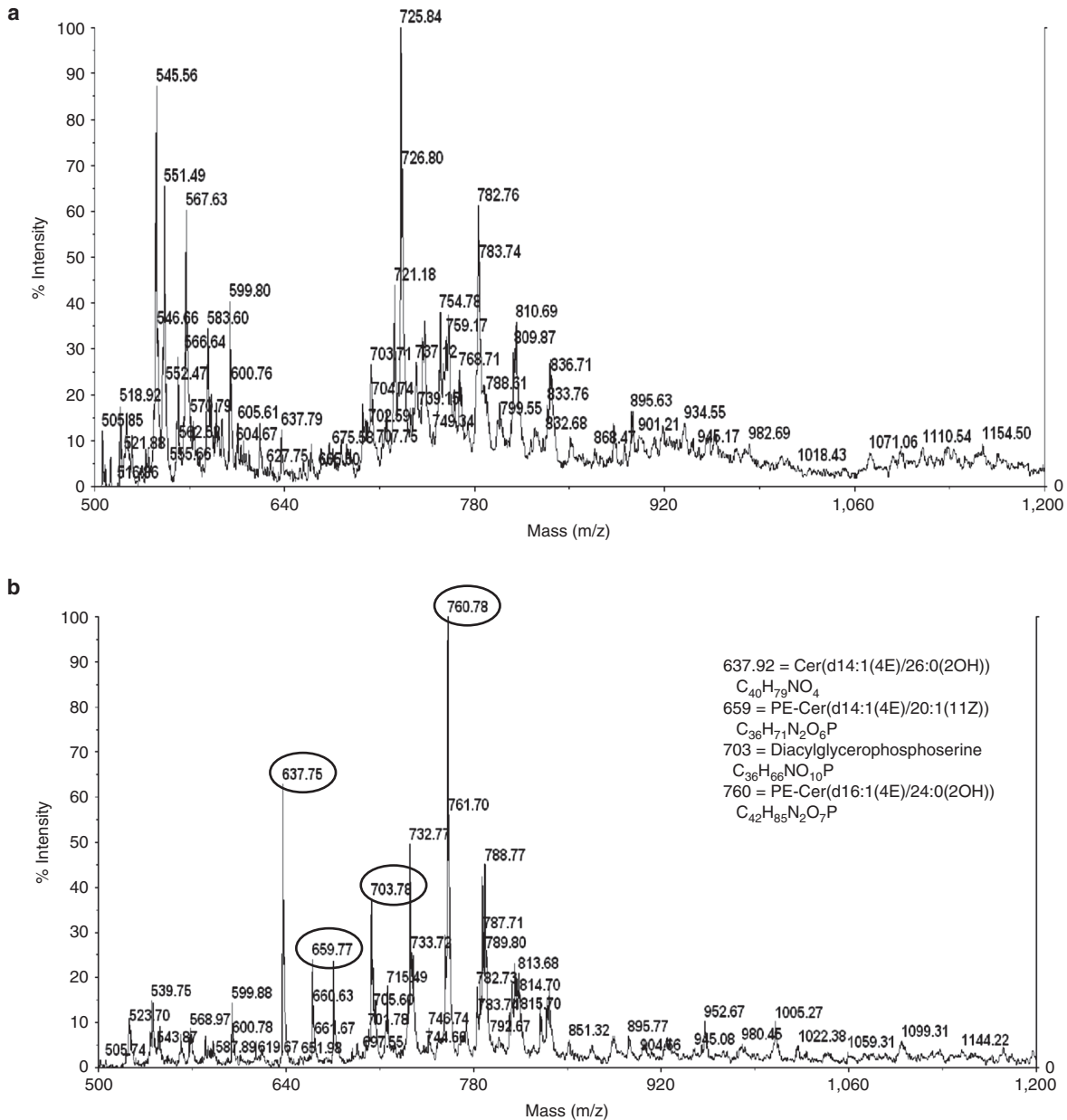


Figure 4 MALDI-TOF mass spectra of cellular lipids. MALDI-TOF mass spectra of chloroform extracts from the HepG2 without (a) and with (b) 5 $\mu\text{mol/l}$ sorafenib incubation. A series of sphingolipid components in the mass range 600–750Da were observed in the cells treated with sorafenib. The identification of sphingolipid was reported in the inset of panel b.

hepatitis.^{26–30} Recent data suggest that serum miRNAs can work also as predictive markers of response to therapy. In fact, serum miRNA expression was recently found to predict the outcome of HCC patients subjected to transarterial chemoembolization. Multivariate analysis demonstrated that α -fetoprotein (AFP), satellite nodules, and miR-425-3p were the independent prognostic factors associated with survival in this cohort of patients.³¹ Sorafenib, a putative multitargeted kinase inhibitor, is the approved targeted therapy for patients with advanced HCC.^{5,6} At least at our knowledge, only one report exists about the correlation between miRNA serum expression and response to sorafenib. In fact, it was recently reported that miRNA 425-3p is a prognosticator in patients

treated with sorafenib.³³ We showed that, in our experimental conditions, the treatment of HCC cells for 72 hours with 5 $\mu\text{mol/l}$ sorafenib induced an increased ceramide accumulation. Over the past decade, several papers have elucidated the roles of ceramide in cell signaling and the potential of modulating this pathway in cancer treatment.^{33,34} Moreover, it was also demonstrated that they induce the incorporation into exosomes and the release of the miRNAs via a ceramide-dependent pathway. Therefore, we hypothesized that sorafenib could modulate the secretion of miRNAs. In fact, among the 84 analyzed generally detectable in serum miRNAs evaluated by qRT-PCR arrays, in the medium of HCC cells treated with sorafenib, we observed a significant

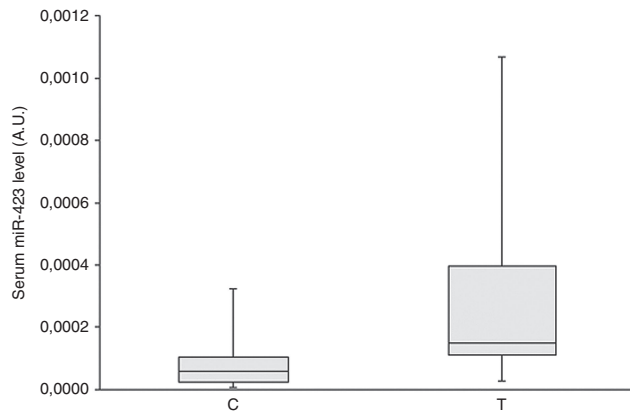


Figure 5 Correlation of serum miR-423 level with Sorafenib therapy. Box plots of serum miR-423 level in 39 patients before (C, control) and after sorafenib therapy (T, treatment). The vertical lines indicate the value ranges; the horizontal boundaries of the boxes represent the first and third quartile. The *P* value for the comparison of the two data sets was 0.006.

increase of miRNA423-5p compared to untreated cells. In addition, we found that the miR-423-5p was increased after sorafenib treatment in serum of 39 HCC patients and in the 75% of patients where it was increased a SD or a PR was recorded. On the basis of these results, we hypothesized that miR-423-5p can play a role in the biology of HCC. To assess this hypothesis, we evaluated the role of miR-423 on proliferation and programmed cells death in miR-423-5p-transfected Huh7 cells. miR-423 overexpression caused an accumulation of HuH-7 cells in S phase paralleled by increased p27 and, at a lesser extent, p21 expression, and decreased phosphorylation of MAPK (Erk-1 and Erk-2) and AKT, key molecules involved in the regulation of both cell proliferation and survival. Moreover, the transfection with miR-423 did not induce any increase of apoptotic cells (data not shown). Interestingly, the increased expression of p21 and p27 was not correlated to an increase of $G_{0/1}$ phase likely because we have not evaluated the kinetic of cell cycle distribution but considered a single time point without on/off labeling experiments. It is possible that at different time points an accumulation of cells in $G_{0/1}$ could be recorded. We used miRanda and TargetScan to identify target oncogenes of miR-423-5p and detected a potential candidate target that was related to cell death. In fact, the analysis revealed that ATG7 (an autophagic protein) was a putative target of miR-423. Previous studies have demonstrated that autophagy can be activated by physiological signals (e.g., starvation), pharmacological agents (e.g., rapamycin), or immunological stimuli, such as Toll-like receptor (TLR) ligands and cytokines (e.g., IFN- γ and TNF).³⁵ The mammalian target of rapamycin (mTOR) plays a key role in inhibiting autophagy,³⁶ and its activity is enhanced by Ras homologue enriched in brain (Rheb).³⁷ Moreover, the expression of autophagic genes and their corresponding autophagic activities are suppressed in some HCC cells, and these defects can be associated with malignant phenotype and poor prognosis of HCC in an apoptosis-compromised background.³⁸ We have demonstrated by FACS, TEM, and western blot that autophagy activation and cell death was induced by overexpression of miR-423. It is also to be considered that

in previous studies miR-423-5p did not induce effects in HepG2 and SNU449 cells. However, our results were obtained in a different cell line and it can not be excluded the different molecular context can have important influence on the molecular interference induced by miRNAs.³⁹

In conclusion, our data suggest that miR-423-5p has a biological role in both cell cycle regulation and autophagy occurrence in HCC cells as showed in **Figure 9**. Preliminary data in the serum of patients affected by HCC after the beginning of treatment with sorafenib showed an early increase of miRNA-423-5p and it was suggested a correlation to response to therapy deserving potential function as predictive biomarker of response to sorafenib. These data strongly warrant additional validation in a larger cohort of patients in order to achieve recommendation as routinely used predictive biomarker.

Materials and Methods

Cell cultures. Human hepatocarcinoma cell line HUH7 obtained from the American Type Tissue Culture Collection, Rockville, MD, were cultured in Dulbecco's modified Eagle's medium supplemented with heat inactivated 10% fetal serum bovine, 20 mmol/l Hepes, 100 U/ml penicillin, 100 μ g/ml streptomycin, and 1% L-glutamine. HepG2 cells were cultured in Dulbecco's modified Eagle's medium supplemented with 10% fetal bovine serum, 100 U/ml of penicillin, and 100 μ g/ml of streptomycin. The cells were grown in a humidified atmosphere of 95% air/5% CO₂ at 37 °C. After incubation for 24 hours in Dulbecco's modified Eagle's medium with 10% fetal bovine serum, the cells were incubated with Sorafenib at a concentration of 5 μ mol/l for 72 hours. All experiments were performed in triplicate.

Patient characteristics, treatment schedule, and isolation of peripheral blood mononuclear cells. A total of 39 patients (31 M/8 F) were enrolled between July 2012 and July 2014. Patients were required to have HCC confirmed by biopsy or diagnosed by radiological and clinical criteria, as previously described.⁴⁰ Patients received sorafenib 400 mg b.i.d. for 28 days. Treatment was continued until disease progression or unacceptable toxicity. Dose reduction of sorafenib (200 mg two times per day (b.i.d.)) and octreotide (20 mg) were allowed for drug-related toxicities (National Cancer Institute Common Toxicity Criteria version 2.0). Response to treatment was assessed by at least two independent radiologists, using RECIST criteria every 2 months. Patients were considered "responsive to the treatment" if a PR or a SD lasting equal or more than 6 months was recorded and "resistant to treatment" if a PR or SD lasting less than 6 months or a PD was recorded. The biological samples were collected before the treatment (T0), and 21 days (T21) from the beginning of the schedule and every month until progression was recorded. Sera were collected from the patients at the selected times and stored at -80 °C for all the following experiments.

Transfection of HUH7 cells with miRNA 423-5p mimic and inhibitor. To establish the specific role of miRNA 423-5p, HUH7 cells at 80% of confluence were transfected with miRNA 423-5p and its inhibitor. The day before transfection, cells were trypsinized and seeded in medium without antibiotics in 12-well plates. MIRIDIAN miR-423-5p mimic,

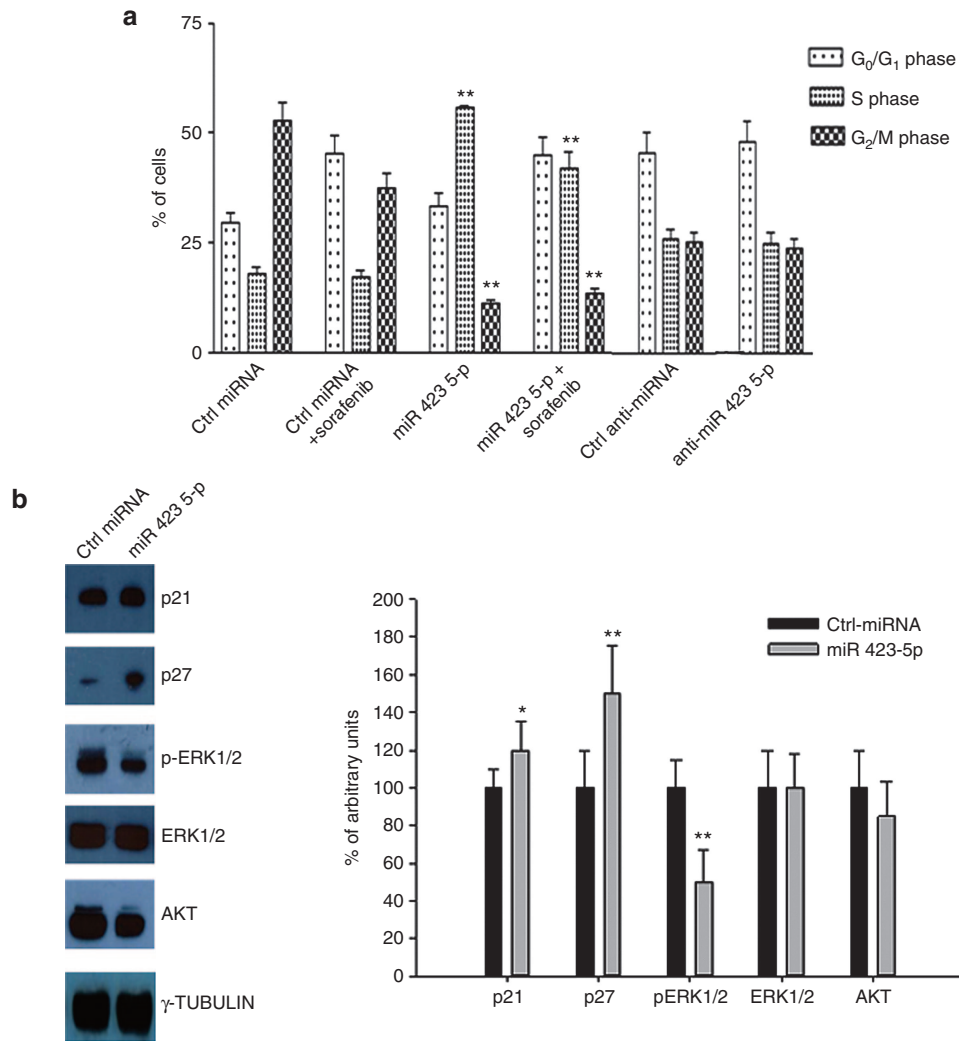


Figure 6 Effects of miRNA 423-5p on cell proliferation and distribution in cell cycle. (a) Cell cycle distribution after 72 hours from transfection with Ctrl-miRNA and miR-423-5p with or without sorafenib (5 $\mu\text{mol/l}$) in HuH-7 cells, evaluated by FACS, as described in Materials and Methods. Data are expressed as mean \pm SD of the percentage of cells in the different phases of the cell cycle, as compared with untreated control cells. Control values have been set to 100%. (b) Effects of transfection with Ctrl miRNA and miR 423-5p on p21, p27, pERK1/2, ERK1/2 AKT expressions in HuH7 cells. γ -tubulin was used as loading control. The intensity of each band was expressed as % arbitrary units compared to that of the Ctrl cells. Error bars showed standard deviation from the mean in at least three independent experiments.

miRIDIAN miR-423-5p hairpin inhibitor, and their controls with unrelated sequences (Dharmacon, Lafayette, CO) were transfected at 50 nmol/l along with 50 ng of phRL-tk plasmid encoding Renilla luciferase to monitor transfection efficiency. Transfections were performed by using Lipofectamine2000 (Invitrogen, Carlsbad, CA), as described by the manufacturer. After 6 hours, transfection mix was replaced with complete medium. The analyses were performed 72 hours after transfection.

Cell proliferation assay. We assessed the viability of the cell lines tested to Sorafenib using a microplate colorimetric assay that measures the ability of viable cells to transform a soluble tetrazolium salt (3-(4,5-Dimethylthiazol-2-yl)-2,5-Diphenyl-tetrazolium Bromide (MTT) to an insoluble purple formazan precipitate. Cells were plated at the appropriate density in 96-well microtitre plates. After 24 hours, cells were exposed to various concentrations of Sorafenib for 24, 48, and 72

hours. Then, 50 μl of MTT (1 mg/ml) and 200 μl of medium were added to the cells in each well. After 4 hours incubation at 37 $^{\circ}\text{C}$, the medium was removed, then the formazan crystals were solubilized by adding 100 μl of Dimethyl sulfoxide (DMSO) and by mixing it in an orbital shaker for 20 minutes. Absorbance at 570 nm was measured using a plate reader. Experiments were performed in triplicate. As a control, 0.5% DMSO was added to untreated cells.

Labeling of autophagic vacuoles with MDC. To quantify the induction of the autophagic process in HUH7 cells transfected with miRNA 423-5p mimic and inhibitor, cells were treated with Sorafenib (5 $\mu\text{mol/l}$) for 72 hours. Following the treatments, cells were incubated with 50 mmol/l MDC (Sigma, Milan, Italy) in phosphate-buffered saline (PBS) at 37 $^{\circ}\text{C}$ for 15 minutes. After incubation, cells were washed with PBS, trypsinized, and immediately analyzed by flow cytometry. All fluorescences were analyzed with a FACScalibur flow

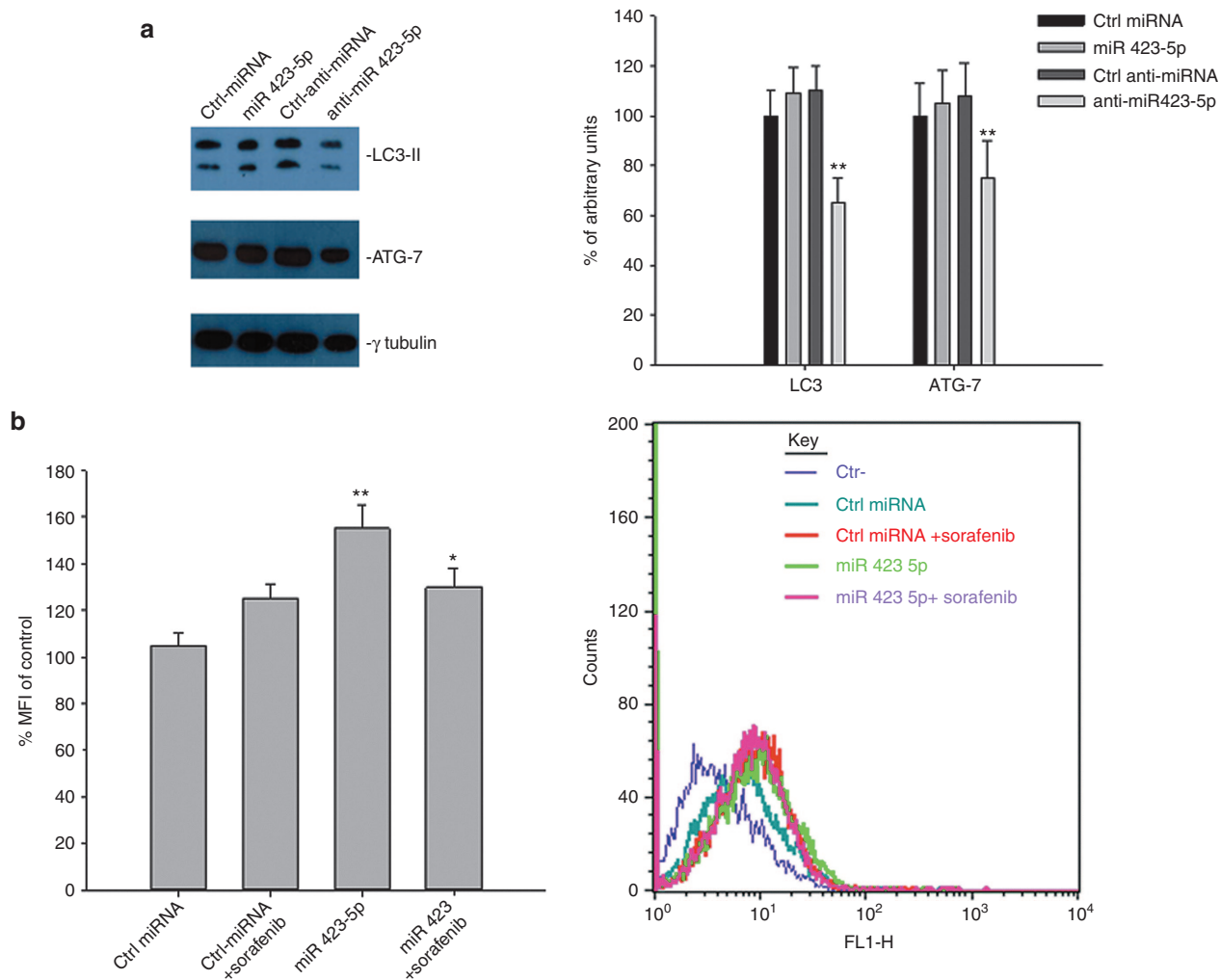


Figure 7 Effects of miR 423-5p on autophagy of hepatocellular carcinoma cells. (a) After transfection with Ctrl miRNA, miR 423-5p, Ctrl anti-miRNA, and anti-miR 423-5p, ATG7 and LC3-II expression was evaluated by western blot assay with specific antibodies as described in “Materials and methods”. The intensities of the bands were expressed as % arbitrary units. Error bars showed standard deviation from the mean in at least three independent experiments. (b) Flow cytometric analyses of autophagosomes formation (MDC incorporation) in HUH-7 cells after 72 hours from transfection with Ctrl-miRNA and miR-423-5p with or without Sorafenib (5 μ mol/l) as described in Materials and Methods. The % mean fluorescence intensities were calculated, as % of untreated control. Values are the means of three independent experiments (\pm SD).

cytometer (Becton Dickinson, San Jose, CA). The fluorescent emissions were collected through a 530nm band pass filter (FL1 channel). At least 10,000 events were acquired in log mode. For the quantitative evaluation of MDC, CellQuest software (Becton Dickinson) was used to calculate MFIs. The MFIs were calculated by the formula (MFI treated/MFI control), where MFI treated is the fluorescence intensity of cells treated with the various compounds and MFI control is the fluorescence intensity of untreated and unstained cells as previously reported.

Cell cycle analysis. HUH7-transfected cells were seeded in 100-mm plates at the density of 1×10^6 cells/plate. After incubation with Sorafenib, cells were washed in PBS, pelleted, and directly stained in a PI solution (50 μ g PI in 0.1% sodium citrate, 0.1% NP40, pH 7.4) for 30 minutes at 4 $^{\circ}$ C in the dark. Flow cytometry analysis was performed using a FACScan flow cytometer (Becton Dickinson). To evaluate cell

cycle PI fluorescence was collected as FL2 (linear scale) by the ModFIT software (Becton Dickinson). For the evaluation of intracellular DNA content, at least 20,000 events for each point were analyzed in at least three different experiments giving an SD less than 5%.

Western blotting. Cells were grown for 72 hours with Sorafenib (5 μ mol/l) at 37 $^{\circ}$ C. For cell extract preparation, the cells were washed twice with ice-cold PBS/ bovine serum albumin (BSA), scraped, and centrifuged for 30 minutes at 4 $^{\circ}$ C in 1 ml of lysis buffer (1% Triton, 0.5% sodium deoxycholate, 0.1 mol/l NaCl, 1 mmol/l Ethylenediaminetetraacetic acid (EDTA), pH 7.5, 10 mmol/l Na_2HPO_4 , pH 7.4, 10 mmol/l phenylmethanesulfonyl fluoride (PMSF), 25 mmol/l benzimidin, 1 mmol/l leupeptin, 0.025 units/ml aprotinin) as previously described.⁴¹ Equal amounts of cell proteins were separated by SDS-PAGE, electrotransferred to nitrocellulose, and reacted with the different antibodies. Blots were then

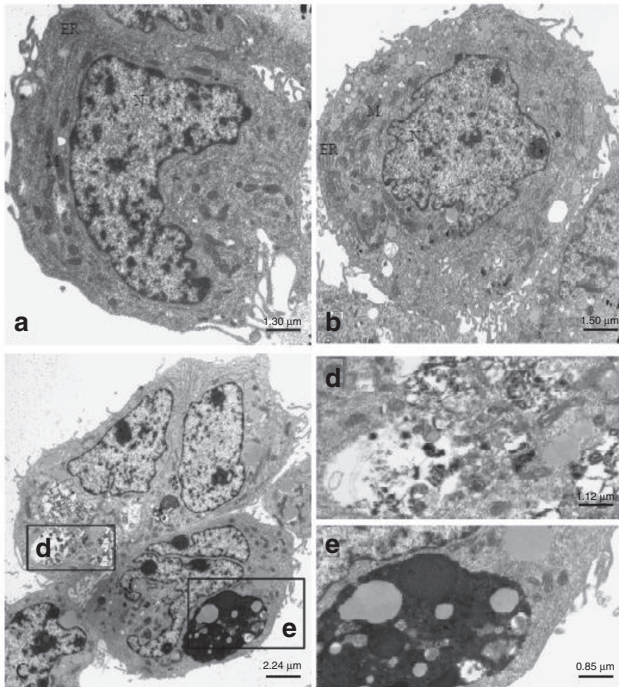


Figure 8 Effects of miR 423-5p on autophagy of hepatocellular carcinoma cells evaluated by TEM. HUH-7 cells transfected with Ctrl-miRNA cells exhibited the ultrastructural morphology of cytoplasm, organelles, and nuclei similar to that of normal hepatocytes (a,b). HUH-7 cells transfected with miR-423-5p for 72 hours developed autophagosome-like characteristics, including single- or double-membrane vacuoles containing intact and degraded cellular debris (c–e).

developed using enhanced chemoluminescence detection reagents (SuperSignal West Pico, Pierce, CA) and exposed to X-ray film. All films were scanned by using Quantity One software (BioRad laboratories, Hercules, CA).

TEM. For ultrastructural study, cells were washed with PBS 1N and then fixed in 2.5% glutaraldehyde in PBS 1N for 2 hours at 4 °C. After washing four times with 1N PBS, the cells were postfixed in 1% osmium tetroxide for 1 hour, dehydrated in graded ethanol for a total of 1 hour 30 minutes, and were then enclosed in Epon 812. Ultrathin sections were collected on nickel grids and stained with 2% uranyl acetate and 0.65% lead citrate for 7 minutes. The TEM observations were carried out at the Anton Dohrn Zoological Station of Naples with a Leo 912 AB electron microscope.

RNA purification. Total RNA, including small RNAs, was extracted from 200 µl of serum using miRNeasy Mini kit (Qiagen, Venlo, Netherlands) according to the supplementary protocol provided for miRNA isolation from serum. The same protocol was applied also to RNA extraction from cell culture medium, after removing cellular debris by centrifuging the conditioned medium at 12,000 × g for 35 minutes at room temperature. A 5-µl aliquot of 5 nmol/l Syn-cel-miRNA-39 miScript miRNA Mimic was spiked into each sample before nucleic acid preparation to monitor the efficiency of miRNA recovery and to normalize miRNA expression in the subsequent real-time PCR.

miRNA profiling and real-time PCR analyses. Aliquots of RNA extracted from the different medium samples conditioned by

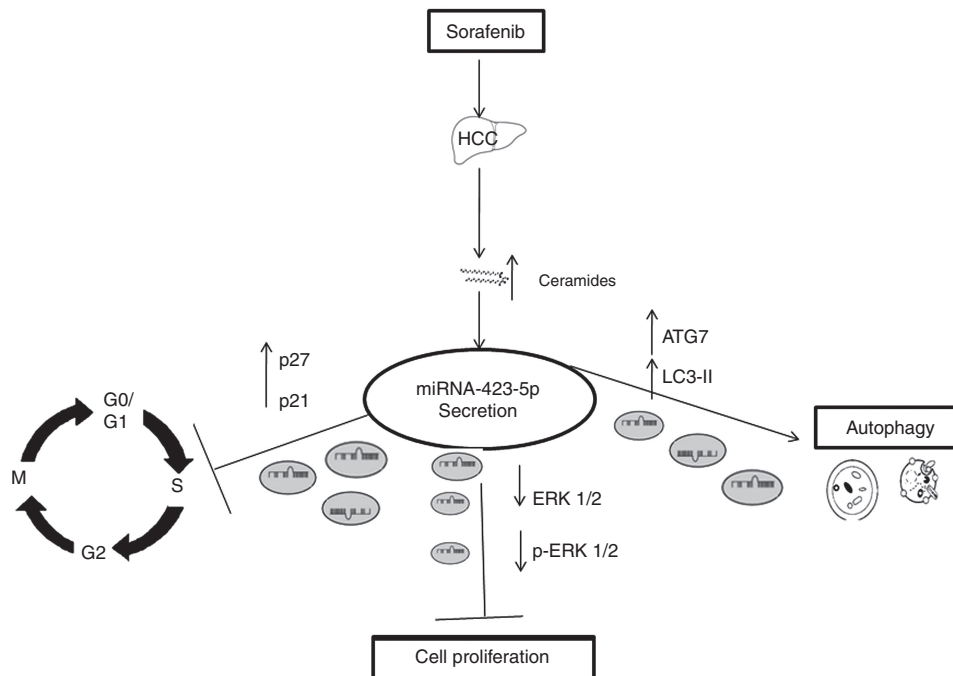


Figure 9 The addition of sorafenib to hepatocellular carcinoma cells increases the intracellular levels of ceramides that, in turn, determines an increased secretion of miR423-5p. The latter induces p21/p27 increase with consequent cell cycle perturbation, reduces pErk-1/2 expression and activity arresting proliferation and triggers autophagy occurrence.

the same number of cells were reverse-transcribed by using miScript II RT kit (SABiosciences, San Francisco, CA); half preparation of cDNA was used for real-time PCR profiling of mature miRNAs using Human Serum&Plasma miRNA PCR Arrays (SABiosciences) in combination with miScript SYBR Green PCR kit (SABiosciences) and the MyiQ2 (Bio-Rad, Hercules, CA) instrument. Data analysis was performed with the web-based software package for the miRNA PCR array system (<http://pcrdataanalysis.sabiosciences.com/mirna/arrayanalysis.php>). In brief, ΔC_t value for each miRNA profiled in a plate is calculated using the formula $\Delta C_t = C_t^{\text{miRNA}} - C_t^{\text{cel-miR-39}}$. $\Delta\Delta C_t$ for each miRNA across the two groups of samples (before and after 72 hour of sorafenib treatment) is calculated using the formula: $\Delta\Delta C_t = \Delta C_t$ of treatment group $- \Delta C_t$ of control group. Expression fold-change was then obtained as $2^{-\Delta\Delta C_t}$ (the normalized gene expression ($2^{-\Delta C_t}$) in the treatment group divided the normalized gene expression ($2^{-\Delta C_t}$) in the control group. Data are reported as fold-regulation, where fold-regulation is equal to the fold-change for fold-change values greater than one (up-regulation) or is the negative inverse of the fold-change for fold-change values lower than one (downregulation). The *P* values are calculated based on a Student's *t*-test of the replicate $2^{-\Delta C_t}$ values for each miRNA in the control and treatment groups and the criteria of differential expression were *P* < 0.05.

cDNA preparations from serum samples and from conditioned medium were then used for real-time PCR analyses using the specific miR-423 miScript Primer Assay (SABiosciences) in combination with miScript SYBR Green PCR kit (SABiosciences). The level of miR-423 in each sample was normalized to cel-miR-39 as described above.

Extraction of lipid and MALDI-TOF MS analysis. Phospholipids were extracted in chloroform–methanol according to Stiuso et al.³⁸ Methanol–chloroform (2: 1 v/v; 800 l) was added to the homogenate of HepG2 with and without treatment for 72 hours with 5 $\mu\text{mol/l}$ sorafenib. Phase separation is induced by adding 200 μl of water. The mixture was centrifuged at 1,000 g for 10 minutes. The upper phase was discarded and the lower chloroform phase was evaporated to dryness under a stream of nitrogen. The lipids were dissolved in 100 μl of chloroform. A 2-l aliquot was used for MALDI-TOF MS determination. MALDI-TOF MS experiments were carried out by loading lipid mixtures (1 ml from a solution 0.02 mg/ml in H₂O/0.1% v/v TFA) on the stainless steel target together with 1 l of matrix 2,5-dihydroxybenzoic acid (10 mg in 1 ml MeOH/0.1% v/v TFA). Spectra were acquired on a PerSeptive Biosystems (Framingham, MA) Voyager DE-PRO mass spectrometer, equipped with a N₂ laser (337 nm, 3 ns pulse width) operating either in linear or in reflector positive ion mode, using the delayed extraction technology. In the analysis of lipids, laser power was maintained at the lowest possible values in order to prevent in-source fragmentation. To check repeatability, spectra were acquired in triplicate at least.

Acknowledgments. M.C. was supported by the Italian Ministry of Education, University and Research (MIUR) with a project (FIRB-ACCORDI DI PROGRAMMA 2011) entitled: “Application of high-throughput technology platforms for the characterization of new biomarkers and molecular targets in

nanovectors for the diagnosis and treatment of human cancer”. M.C. was supported by Regione Campania with a project entitled “Laboratori Pubblici Progetto Hauteville”. We thank Stazione Zoologica “Anton Dohrn” and CISME of University of Naples “Federico II” for technical assistance at TEM.

- Parkin, DM, Bray, F, Ferlay, J and Pisani, P (2005). Global cancer statistics, 2002. *CA Cancer J Clin* **55**: 74–108.
- Llovet, JM (2005). Updated treatment approach to hepatocellular carcinoma. *J Gastroenterol* **40**: 225–235.
- Rossi, M, Rotblat, B, Ansell, K, Amelio, I, Caraglia, M, Misso, G et al. (2014). High throughput screening for inhibitors of the HECT ubiquitin E3 ligase ITCH identifies antidepressant drugs as regulators of autophagy. *Cell Death Dis* **5**: e1203.
- Vitale, G, Zappavigna, S, Marra, M, Dicitore, A, Meschini, S, Condello, M et al. (2012). The PPAR- γ agonist troglitazone antagonizes survival pathways induced by STAT-3 in recombinant interferon- β treated pancreatic cancer cells. *Biotechnol Adv* **30**: 169–184.
- Llovet, JM, Ricci, S, Mazzaferro, V, Hilgard, P, Gane, E, Blanc, JF et al.; SHARP Investigators Study Group. (2008). Sorafenib in advanced hepatocellular carcinoma. *N Engl J Med* **359**: 378–390.
- Forner, A, Hessheimer, AJ, Isabel Real, M and Bruix, J (2006). Treatment of hepatocellular carcinoma. *Crit Rev Oncol Hematol* **60**: 89–98.
- Yau, T, Chan, P, Epstein, R and Poon, RT (2009). Management of advanced hepatocellular carcinoma in the era of targeted therapy. *Liver Int* **29**: 10–17.
- Llovet, JM and Bruix, J (2003). Systematic review of randomized trials for unresectable hepatocellular carcinoma: Chemoembolization improves survival. *Hepatology* **37**: 429–442.
- Thorgeirsson, SS and Grisham, JW (2002). Molecular pathogenesis of human hepatocellular carcinoma. *Nat Genet* **31**: 339–346.
- Miska, EA (2005). How microRNAs control cell division, differentiation and death. *Curr Opin Genet Dev* **15**: 563–568.
- Watanabe, Y and Kanai, A (2011). Systems Biology Reveals MicroRNA-Mediated Gene Regulation. *Front Genet* **2**: 29.
- Jiang, YW and Chen, LA (2012). microRNAs as tumor inhibitors, oncogenes, biomarkers for drug efficacy and outcome predictors in lung cancer (review). *Mol Med Rep* **5**: 890–894.
- Mitchell, PS, Parkin, RK, Kroh, EM, Fritz, BR, Wyman, SK, Pogosova-Agadjanyan, EL et al. (2008). Circulating microRNAs as stable blood-based markers for cancer detection. *Proc Natl Acad Sci USA* **105**: 10513–10518.
- Chen, X, Ba, Y, Ma, L, Cai, X, Yin, Y, Wang, K et al. (2008). Characterization of microRNAs in serum: a novel class of biomarkers for diagnosis of cancer and other diseases. *Cell Res* **18**: 997–1006.
- Zhou, J, Yu, L, Gao, X, Hu, J, Wang, J, Dai, Z et al. (2011). Plasma microRNA panel to diagnose hepatitis B virus-related hepatocellular carcinoma. *J Clin Oncol* **29**: 4781–4788.
- Toffanin, S, Hoshida, Y, Lachenmayer, A, Villanueva, A, Cabellos, L, Minguez, B et al. (2011). MicroRNA-based classification of hepatocellular carcinoma and oncogenic role of miR-517a. *Gastroenterology* **140**: 1618–28.e16.
- Misso, G, Di Martino, MT, De Rosa, G, Farooqi, AA, Lombardi, A, Campani, V et al. (2014). Mir-34: a new weapon against cancer? *Mol Ther Nucleic Acids* **3**: e194.
- Marfella, R, Di Filippo, C, Potenza, N, Sardu, C, Rizzo, MR, Siniscalchi, M et al. (2013). Circulating microRNA changes in heart failure patients treated with cardiac resynchronization therapy: responders vs. non-responders. *Eur J Heart Fail* **15**: 1277–1288.
- Augello, C, Vaira, V, Caruso, L, Destro, A, Maggioni, M, Park, YN et al. (2012). MicroRNA profiling of hepatocarcinogenesis identifies C19MC cluster as a novel prognostic biomarker in hepatocellular carcinoma. *Liver Int* **32**: 772–782.
- Ma, Y, Wang, R, Zhang, J, Li, W, Gao, C, Liu, J et al. (2014). Identification of miR-423 and miR-499 polymorphisms on affecting the risk of hepatocellular carcinoma in a large-scale population. *Genet Test Mol Biomarkers* **18**: 516–524.
- Giray, BG, Emekdas, G, Tezcan, S, Ulger, M, Serin, MS, Sezgin, O et al. (2014). Profiles of serum microRNAs; miR-125b-5p and miR223-3p serve as novel biomarkers for HBV-positive hepatocellular carcinoma. *Mol Biol Rep* **41**: 4513–4519.
- Kosaka, N, Iguchi, H, Yoshioka, Y, Takeshita, F, Matsuki, Y and Ochiya, T (2010). Secretory mechanisms and intercellular transfer of microRNAs in living cells. *J Biol Chem* **285**: 17442–17452.
- Resnick, KE, Alder, H, Hagan, JP, Richardson, DL, Croce, CM and Cohn, DE (2009). The detection of differentially expressed microRNAs from the serum of ovarian cancer patients using a novel real-time PCR platform. *Gynecol Oncol* **112**: 55–59.
- Yamamoto, Y, Kosaka, N, Tanaka, M, Koizumi, F, Kanai, Y, Mizutani, T et al. (2009). MicroRNA-500 as a potential diagnostic marker for hepatocellular carcinoma. *Biomarkers* **14**: 529–538.
- Tan, Y, Ge, G, Pan, T, Wen, D, Chen, L, Yu, X et al. (2014). A serum microRNA panel as potential biomarkers for hepatocellular carcinoma related with hepatitis B virus. *PLoS ONE* **9**: e107986.
- Meng, FL, Wang, W and Jia, WD (2014). Diagnostic and prognostic significance of serum miR-24-3p in HBV-related hepatocellular carcinoma. *Med Oncol* **31**: 177.
- Zhang, ZQ, Meng, H, Wang, N, Liang, LN, Liu, LN, Lu, SM et al. (2014). Serum microRNA 143 and microRNA 215 as potential biomarkers for the diagnosis of chronic hepatitis and hepatocellular carcinoma. *Diagn Pathol* **9**: 135.

28. Ge, W, Yu, DC, Li, QG, Chen, X, Zhang, CY and Ding, YT (2014). Expression of serum miR-16, let-7f, and miR-21 in patients with hepatocellular carcinoma and their clinical significances. *Clin Lab* **60**: 427–434.
29. Coppola, N, Potenza, N, Pisaturo, M, Mosca, N, Tonziello, G, Signoriello, G et al. (2013). Liver microRNA hsa-miR-125a-5p in HBV chronic infection: correlation with HBV replication and disease progression. *PLoS ONE* **8**: e65336.
30. Liu, M, Liu, J, Wang, L, Wu, H, Zhou, C, Zhu, H et al. (2014). Association of serum microRNA expression in hepatocellular carcinomas treated with transarterial chemoembolization and patient survival. *PLoS ONE* **9**: e109347.
31. Vaira, V, Roncalli, M, Carnaghi, C, Favarsani, A, Maggioni, M, Augello, C et al. (2015). MicroRNA-425-3p predicts response to sorafenib therapy in patients with hepatocellular carcinoma. *Liver Int* **35**: 1077–1086.
32. Caraglia, M, Giuberti, G, Marra, M, Addeo, R, Montella, L, Murolo, M et al. (2011). Oxidative stress and ERK1/2 phosphorylation as predictors of outcome in hepatocellular carcinoma patients treated with sorafenib plus octreotide LAR. *Cell Death Dis* **2**: e150.
33. Kolesnick, R (2002). The therapeutic potential of modulating the ceramide/sphingomyelin pathway. *J Clin Invest* **110**: 3–8.
34. Canals, D, Perry, DM, Jenkins, RW and Hannun, YA (2011). Drug targeting of sphingolipid metabolism: sphingomyelinases and ceramidases. *Br J Pharmacol* **163**: 694–712.
35. Wang, J, Yang, K, Zhou, L, Minhaowu, Wu, Y, Zhu, M et al. (2013). MicroRNA-155 promotes autophagy to eliminate intracellular mycobacteria by targeting Rheb. *PLoS Pathog* **9**: e1003697.
36. Levine, B, Mizushima, N and Virgin, HW (2011). Autophagy in immunity and inflammation. *Nature* **469**: 323–335.
37. Ding, ZB, Shi, YH, Zhou, J, Qiu, SJ, Xu, Y, Dai, Z et al. (2008). Association of autophagy defect with a malignant phenotype and poor prognosis of hepatocellular carcinoma. *Cancer Res* **68**: 9167–9175.
38. Calvisi, DF, Ladu, S, Gorden, A, Farina, M, Lee, JS, Conner, EA et al. (2007). Mechanistic and prognostic significance of aberrant methylation in the molecular pathogenesis of human hepatocellular carcinoma. *J Clin Invest* **117**: 2713–2722.
39. Lin, J, Huang, S, Wu, S, Ding, J, Zhao, Y, Liang, L et al. (2011). MicroRNA-423 promotes cell growth and regulates G1/S transition by targeting p21Cip1/Waf1 in hepatocellular carcinoma. *Carcinogenesis* **32**: 1641–1647.
40. Stiuso, P, Scognamiglio, I, Murolo, M, Ferranti, P, De Simone, C, Rizzo, MR et al. (2014). “Serum Oxidative Stress Markers and Lipidomic Profile to Detect NASH Patients Responsive to an Antioxidant Treatment: A Pilot Study”. *Oxidative Med Cell Longev* **2014**: 131024.
41. Esposito, F, Boscia, F, Franco, R, Tornincasa, M, Fusco, A, Kitazawa, S et al. (2011). Down-regulation of oestrogen receptor- β associates with transcriptional co-regulator PATZ1 delocalization in human testicular seminomas. *J Pathol* **224**: 110–120.



This work is licensed under a Creative Commons Attribution-NonCommercial-NoDerivs 4.0 International License. The images or other third party material in this article are included in the article's Creative Commons license, unless indicated otherwise in the credit line; if the material is not included under the Creative Commons license, users will need to obtain permission from the license holder to reproduce the material. To view a copy of this license, visit <http://creativecommons.org/licenses/by-nc-nd/4.0/>